

# THREE-DIMENSIONAL RECONSTRUCTION AND CHARACTER EXTRACTION OF CORN PLANTS BASED ON KINECT SENSOR

## 基于Kinect传感器的玉米植株三维重构与性状提取

Yuanyuan SUN<sup>1)</sup>, Xuchang WANG<sup>\*2)</sup>, Kaixing ZHANG<sup>3)</sup>

<sup>1)</sup> College of Modern Equipment Academy, Changzhou Vocational Institute of Industry Technology, Changzhou / China;

<sup>2)</sup> Yantai CIMC Raffies Offshore Ltd, Yantai / China;

<sup>3)</sup> College of Mechanical and Electronic Engineering, ShanDong Agricultural University, Tai'an / China

E-mail: s18853853891@163.com

Corresponding author: Xuchang Wang

DOI: <https://doi.org/10.35633/inmateh-69-61>

**Keywords:** Kinect sensor, 3D reconstruction, point cloud segmentation, ellipse fitting, growth parameters

### ABSTRACT

Aiming at the problems of low precision, strong subjectivity, and continuous measurement in the current measurement methods of corn phenotypic traits, a method of measuring corn phenotypic traits with high precision, low cost, easy carrying and continuous measurement was proposed. Firstly, the three-dimensional scanning device Kinect 2.0 is used to collect corn information and process and reconstruct the collected point cloud. Then, the stem and leaf point clouds were segmented by straight-through filtering, ellipse fitting and region growth segmentation. Finally, the phenotypic parameters of corn were obtained by triangulation and plane fitting for the segmented corn leaves, and the accuracy was analyzed. The results showed that the accuracy of corn plant height was 97.622 %, the average relative error of stem long axis was 9.46 %, the average relative error of stem short axis was 11.17 %, and the accuracy of leaf area was 95.577 %. Studies have shown that this method provides a new method for continuous measurement of phenotypic traits in corn.

### 摘要

针对目前玉米表型性状测量方法存在精度低, 主观性强, 不能连续性测量等问题, 提出一种精确度高、耗费少、便携且可连续性测量的玉米表型性状测量方法。首先, 采用三维扫描设备Kinect 2.0 采集玉米信息并对采集后的点云进行处理和三维重建。然后, 利用直通滤波、椭圆拟合、区域增长分割方法分割出玉米茎秆叶片等数据。最后, 对分割后的玉米叶片等利用三角面片化以及平面拟合等方法获取玉米植株表型参数并对其进行精度分析。结果表明: 算法测量株高精确度为97.622%, 茎秆长轴的平均测量相对误差为9.46%, 茎秆短轴平均测量相对误差为11.17%, 叶片面积精确度为95.577%。研究表明, 本文方法为玉米的表型性状测量提供一种连续性测量新方法。

### INTRODUCTION

Corn is an important food crop and an important source of feed. Accurate acquisition of phenotypic traits such as plant height, stem diameter, leaf perimeter and area in the process of corn growth is of great significance for understanding crop growth, yield estimation, disease resistance detection and breeding (Zila Jia *et al*, 2019). Traditional crop phenotypic traits are mainly measured manually. This method is inefficient, has no uniform measurement standard, and cannot continuously measure crops (Yingbo Song, 2015; Jay S., 2015). With the development of industry, researchers began to apply image processing and machine vision for crop phenotype detection. Hui quantified and evaluated the canopy structure of plant populations in two and three dimensions using multi-view stereo (MVS) techniques, and monitored plant growth and development from seedling to fruiting stage. (Hui *et al*, 2018). He *et al*. built a set of multi-view stereo imaging system, collected 360° image data of strawberry fruit, carried out three-dimensional reconstruction, and extracted character parameters (He *et al*, 2017). Aksoy constructed an imaging system using a robotic arm and cameras to monitor different tobacco plants, measuring their growth parameters and leaf growth rates (Aksoy E.E. *et al*, 2015).

---

Yuanyuan Sun, Lecture M.S. Eng.; Xuchang Wang<sup>\*</sup>, Engineer M.S. Eng.; Kaixing Zhang, Prof. Ph.D. Eng.

Based on the structured light scanner, Li obtained the three-dimensional point cloud of cotton, reconstructed the three-dimensional model, and measured the phenotypic traits (Yaochen Li, 2019). Qian Wu realized the recognition and segmentation of overlapping fruits by using color features and three-dimensional geometric features through Kinect v2, which provided an important reference for the research on robotic fruit picking (Qian Wu, 2022). WU used Kinect v2 sensor to obtain multi-view images of rice, and carried out three-dimensional reconstruction of rice plants by contour projection and inverse projection methods (WU D, 2020). Jie Ding proposed a modeling method for rotationally symmetric objects based on Kinect. For rotationally symmetric objects with weak structures, the model can be obtained by rotating fitting boundary (Jie Ding, 2019).

At present, the instruments and technologies for crop 3D reconstruction based on point cloud include Lidar, multi-eye stereo camera, TOF (Time of flight) camera, etc. Kinectv2 sensor is widely used in information agriculture because it has the function of real-time synchronous acquisition of depth information and color information, and has the advantages of good precision, low cost and good compatibility. Measurements based on two-dimensional images are often inaccurate due to occlusion between plants and are not suitable for measuring morphological parameters such as leaf area. Due to the special shape of corn, general trait measurement method is not applicable to it. Therefore, this paper proposes a three-dimensional reconstruction method based on Kinect 2.0 and a phenotypic parameter extraction method based on ellipse fitting for corn. Through experimental verification, the method proposed in this study can extract crop phenotypic parameters non-destructively and accurately, which is of great significance for understanding crop growth status, crop detection, yield estimation, disease resistance detection and breeding.

## MATERIALS AND METHODS

### Experimental Materials and Data Acquisition

The hardware measurement system for corn collection is mainly composed of six parts: control host, Kinect 2.0, tripod, disc and controller. The turntable system is shown in Fig. 1. Capturing the corn plant point cloud scene with Kinect is shown in Fig. 2.

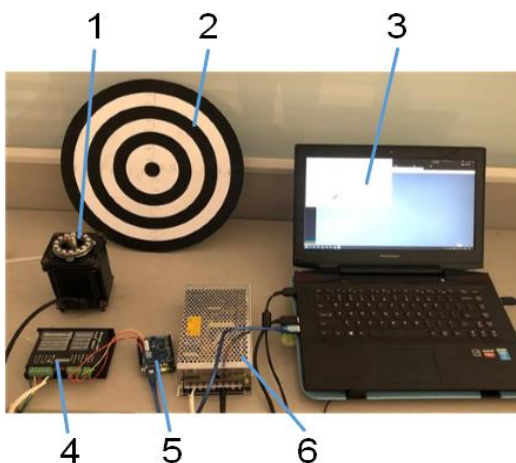


**Fig. 1 - Schematic diagram of measurement composition**

1-Stepper motor; 2-Disc; 3-Control host; 4-Driver;  
5-Arduino control board; 6-Switching power supply



**Fig. 2 - Acquisition of corn point cloud data**

1-Collection objects; 2-Disc; 3-Kinect 2.0;  
4-Control host; 5-Tripod

Based on the Windows 10 operating system, this study used the turntable method to scan the corn information. Within the effective range of Kinect v2 (0.5m ~ 5.0m) (Jin Zhou, 2013), the closer the distance is, the higher the accuracy will be. Therefore, under the premise of meeting the use conditions, it should be as close to the corn as possible. The rotation angle was 36°, and the rotation was 9 times to obtain all the information of the corn plant. Based on Kinect 2.0, the color information and depth information of corn plant are obtained and converted into color image and depth image. The depth coordinate space (512 × 424) and color coordinate space (1920 × 1080) of Kinect are registered by using the principle of coordinate system conversion and converted into 3D color point cloud. Fig. 3 is the obtained color depth map.

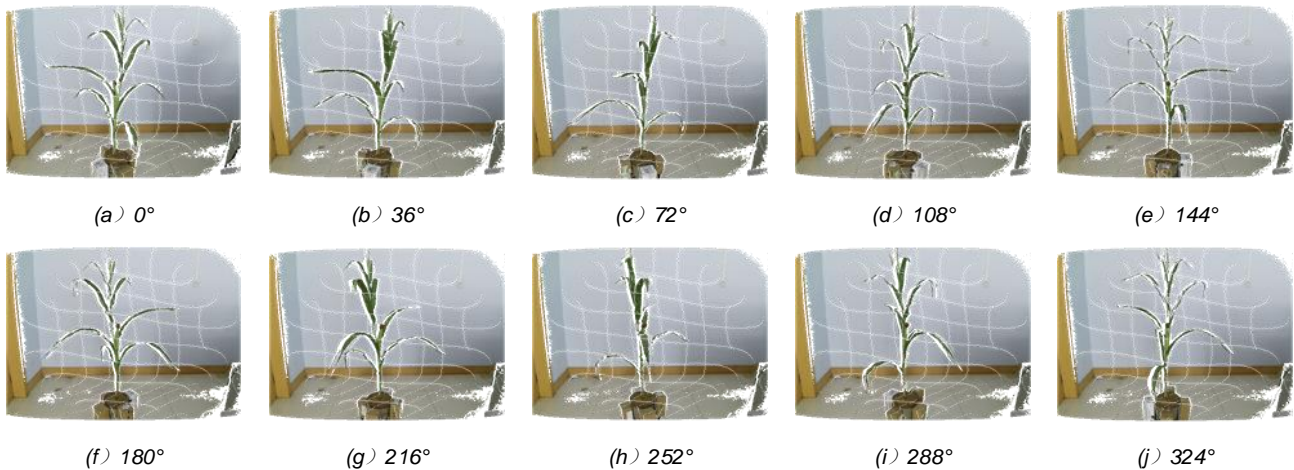


**Fig. 3 - Color depth map obtained from ten directions**

### **Three-dimensional reconstruction of corn**

#### **(1) Point cloud data noise reduction**

Due to the uneven surface of corn leaves and the presence of small villi, the reflection of light will be affected to produce noise points. Noise points will affect the accuracy of 3D reconstruction (Gang Liu *et al*, 2022; Song Bi *et al*, 2021). The obtained corn background point cloud is removed by direct filtering (Archibald R. *et al*, 2019). For the noise points around the point cloud model, this study uses a statistical filtering method to remove them. The idea of statistical filtering is to traverse all point clouds in the point cloud model, and judge whether the point needs to be deleted by the average distance from all points to their neighborhood points. The ten directional point clouds after statistical filtering are shown in Fig. 4. From Fig. 4, it can be seen that the noise points around the target point cloud after statistical filtering are deleted, which improves the accuracy of the point cloud model.

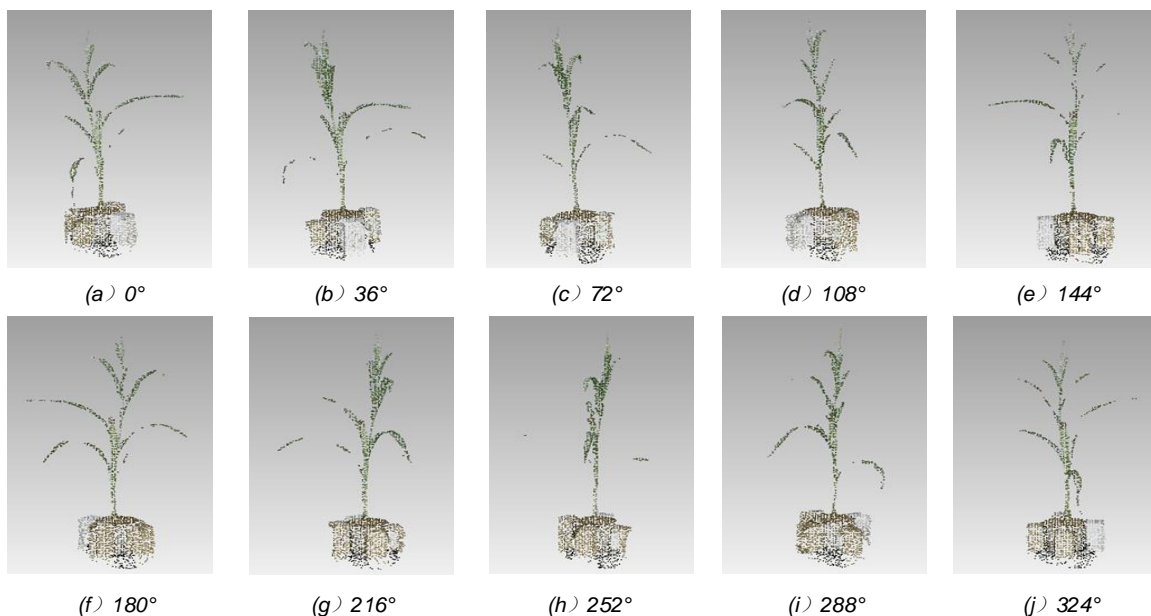


**Fig. 4 - Ten direction point clouds after statistical filtering**

#### **(2) Point cloud matching and simplification**

The local point cloud registration is carried out by manual registration for coarse registration and Iterative Closest Point (ICP) algorithm for fine registration. Before manual coarse registration of point clouds, two adjacent point cloud sets are selected, and four distant feature points are selected from the two point cloud sets for coarse registration.

At this time, the two point cloud sets roughly coincide. In order to reduce the error and improve the registration accuracy, the ICP algorithm is used to perform fine registration. The ICP algorithm finds the corresponding points of two matching point clouds by iteration or search. The Euclidean distance is used as the objective function to iterate continuously, and the rotation matrix and translation matrix of the point cloud are obtained to minimize the error function of the registration point cloud, the point cloud matching of corn is shown in Fig. 5.

The point cloud data after matching is redundant, and too much point cloud data will affect the processing speed and the accuracy of phenotype parameter extraction. Commonly used point cloud simplification methods include curvature-based simplification, random sampling simplification, and bounding box method. The point cloud data after matching is streamlined based on the above method, and the results are shown in Fig. 6. Fig. 6(a) shows the results of curvature-based simplification, with a simplification rate of 30%. The simplified point cloud and the leaf boundary information are seriously lost, and the distribution of leaf point cloud is uneven, which affects the accuracy of the subsequent triangular mesh generation of corn leaves. Fig. 6(b) shows the results of random sampling simplification. The simplification rate is 30%, and there is loss of corn leaf boundary point cloud. Fig. 6(c) shows the simplification of corn plant based on bounding box method, and the simplification spacing is 0.0078. After simplification, the point cloud feature of corn retains the feature information of leaf vein and leaf edge, and the point cloud distribution is relatively uniform, which is convenient for leaf triangular surface to calculate leaf area.



**Fig. 5 - Effect diagram of point clouds registration**

**Fig. 6 - Effect diagram of Point cloud simplification**

(a) Curvature-based simplification (b) Random sampling simplification  
(c) Bounding box method

In summary, the simplification of corn plants based on bounding box method can retain more phenotypic characteristics when the number of point clouds is similar, and the point cloud distribution is uniform, which is convenient for subsequent leaf triangular patching. Therefore, this study selected bounding box method for corn plant point cloud simplification.

### **Segmentation of corn point clouds**

During data acquisition, the Kinect 2.0 uses its own inherent coordinate system to generate three-dimensional point clouds. The principal component direction of the model is inconsistent with the direction of the three-dimensional coordinate axis. Therefore, before the point cloud processing, the point cloud centroid is rotated to the coordinate origin position, so that the corn stalk is along the z-axis direction. Based on the z-axis information, the target point cloud is divided into corn plants and flower pot, and the segmentation effect is shown in Fig. 7 (a).

#### **(1) Ellipse fitting of corn stalk**

In this paper, six-point clouds are selected for ellipse fitting based on the least square method, and all point clouds are traversed to calculate the distance between the point cloud data and the fitting ellipse. When the distance is less than the set threshold, the point is considered to be a standard point. When the distance between all point clouds and the fitting ellipse is calculated, the number of standard points is counted. Repeat the above process until the remaining point cloud is less than six.

Compare the number of point clouds satisfied after each fit. The fitting when the number of point clouds is the largest is the optimal ellipse fitting, and the optimal ellipse fitting parameters are obtained. According to the fitting ellipse, the point cloud of the corn plant point cloud inside the ellipse is extracted, and the segmentation effect is shown in Fig. 7(b).

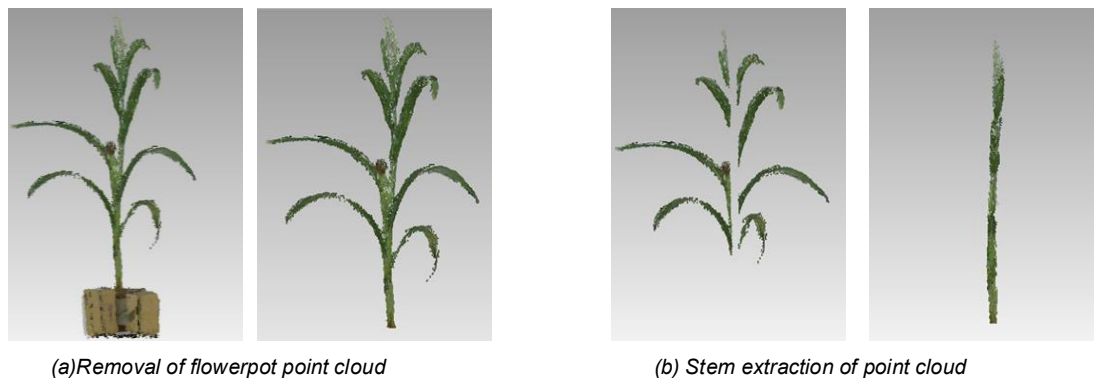


Fig. 7 - Segmentation of Corn point cloud

## (2) Region growing segmentation algorithm

Before the leaf segmentation, the topological relationship of the point cloud is established to search the point cloud, and the point with the smallest curvature is selected as the initial point. Several neighborhood points of the initial point are calculated, and whether these neighborhood points can meet the established growth rules is judged. If the growth rules are met, the search point is classified into the region and used as a new sub-seed point. If only the angle between the seed point and the normal vector of the neighborhood point is within the set threshold range, the neighborhood point is only classified into the same region. Traverse all point clouds and repeat the previous step to continuously add new seed points until no new seed points appear. Repeat the above operation process until all point clouds are divided. The principle of region growing segmentation algorithm is shown in Fig. 8. The segmentation results are represented by different colors, and different colors represent different classes. The segmentation effect is shown in Fig. 9.

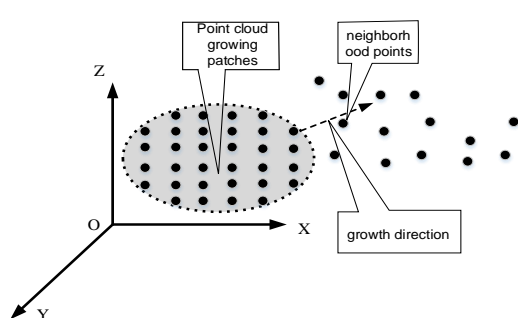


Fig. 8 - Schematic diagram of region growing segmentation algorithm

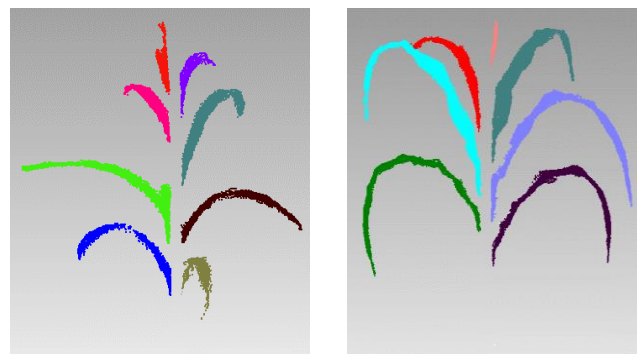


Fig. 9 - Corn point clouds after leaf segmentation

## Extraction and accuracy analysis of corn phenotypic parameters

### (1) Height measurement of corn

The direction of corn stover after coordinate transformation is along the Z-axis. For the corn point cloud after removing the pot, traverse all the points to get the height of the corn plant, namely the Z-coordinate distance between the highest point and the lowest point of the corn plant. The schematic diagram of corn height extraction is shown in Fig. 10.

### (2) Measurement of corn stalk

The stalk diameter of corn can be represented by a fitted elliptic feature, as shown in Fig. 11. The stalk diameter of corn can be calculated according to the long axis and the short axis.

The long and short axes of the fitting ellipse are as follows:

$$\begin{cases} X = \frac{BE - 2CD}{4AC - B} \\ Y = \frac{BD - 2AE}{4AC - B} \end{cases} \quad (1)$$

$$\begin{cases} L = \frac{2(AX + CY + BXY - 1)}{A + C + \sqrt{(A - C) + B}} \\ S = \frac{2(AX + CY + BXY - 1)}{A + C - \sqrt{(A - C) + B}} \end{cases} \quad (2)$$

Where:

$X_c$  and  $Y_c$  are the  $X$  and  $Y$  coordinates of the ellipse center;  
 $L$  and  $S$  are the long half axis and short half axis of ellipse respectively;  
 $A, B, C$  are parameters of fitting elliptic equation.

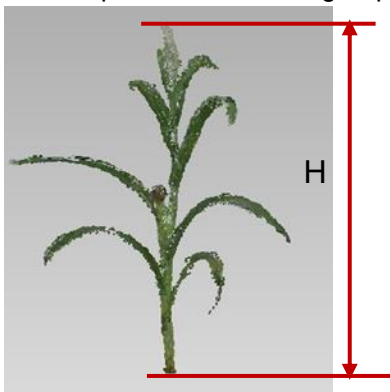


Fig. 10 - Height measurement of corn

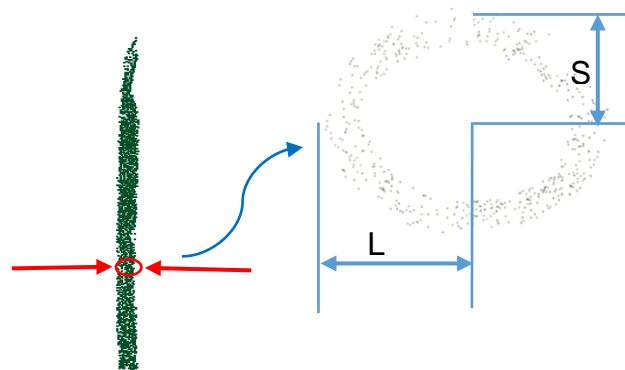
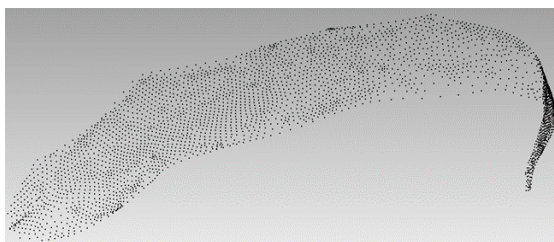


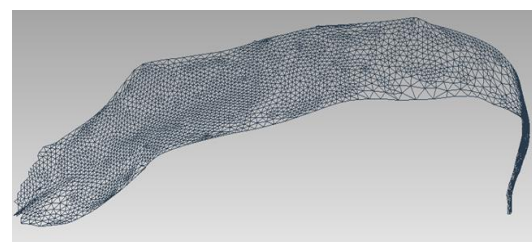
Fig. 11 - Schematic diagram of corn stalk diameter extraction

(3) Measurement of leaf circumference and area of corn

Since the obtained three-dimensional point cloud is scattered points, it cannot display the surface information of the crop directly obtained. Therefore, it is necessary to triangulate the point cloud greedy projection. The threshold of triangular patching is set as follows: the maximum plane angle is  $45^\circ$ , and the maximum angle and minimum angle of each triangle are  $10^\circ$  and  $150^\circ$  respectively. The point cloud of corn leaves is triangularized as shown in Fig. 12(a), and the effect is shown in Fig. 12(b).



(a) Leaf point cloud



(b) Triangulation of leaf point clouds

Fig. 12 - Greedy Projection Triangulation

The three-dimensional point clouds of the blade are transformed into triangular patches with topological relations by greedy projection triangulation algorithm (Hui Chen et al., 2021). The corn leaf model is composed of several small triangles. Each triangle contains the original three-dimensional point cloud information. The side length of the three sides of the triangle is calculated by the vertex coordinates of the triangle, and then the triangle area can be calculated by Helen formula. The area of each triangle is calculated by traversing all triangles in the corn leaf model, and then the area of all triangles is summed to get the corn leaf area.

Helen's formula and the area sum formula are as follows:

$$S_i = \sqrt{p_i(p_i - a_i)(p_i - b_i)(p_i - c_i)} \tag{3}$$

$$S = \sum_{i=1}^n S_i \tag{4}$$

Where:

- $S$  is corn leaf area;
- $S_i$  is the area of the  $i^{th}$  small triangle;
- $p_i$  is half of the area of the  $i^{th}$  triangle;
- $a_i, b_i, c_i$  are the length of three sides of the triangle;
- $n$  is the total number of patches;
- $i$  is the number of face index.

The artificial measurement of corn leaves is to cut the corn leaves with scissors, spread the leaves and place them on the whiteboard. At the same time, a black circle with a diameter of 1 cm is placed on the whiteboard, and a camera is used to shoot in the vertical direction of the whiteboard to obtain images containing corn leaves and circles. Based on the image processing module in Matlab, the circumference and area of corn leaves are calculated, as shown in Fig. 13.

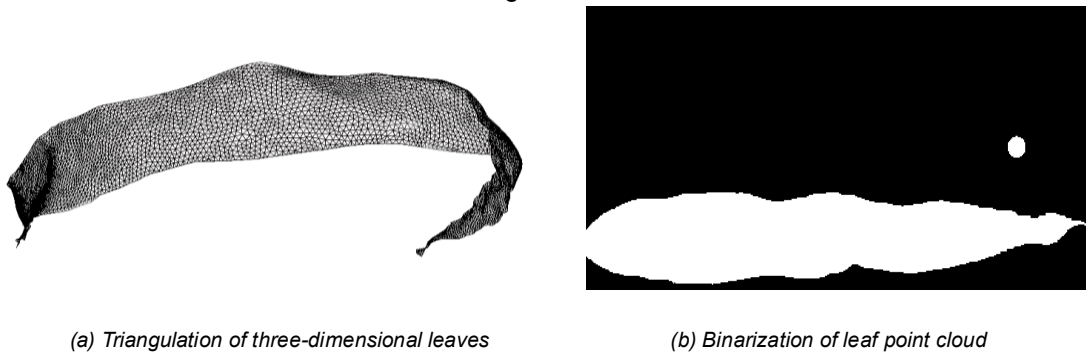


Fig. 13 - Treatment of leaves

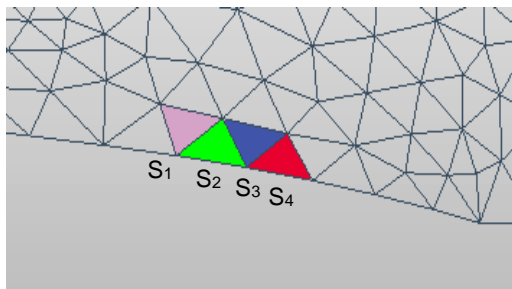


Fig. 14 - Example diagram of boundary triangle

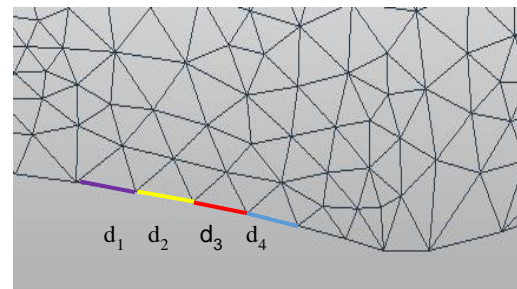


Fig. 15 - Diagram of side length

Retrieve all triangles to find the corn leaf boundary triangle that has two sides with other triangles triangle, they do not share with other triangles side length is added, the result is the blade circumference. The boundary triangles are red and yellow triangles in the corn boundary triangles as in Fig. 14, and the boundary triangles are not co-edges with other triangles such as  $d_1, d_2, d_3, d_4$  in Fig. 15.

**RESULTS**

The effective detection range of Kinect v2 is 0.5~4.5 m, the vertical direction Angle is 60 degrees, and the detection range is within 3.5 to achieve a good effect. At this time, the maximum object collected is 4 meters, which fully meets the information collection requirements of corn in each growth period. The accuracy of the measurement of the phenotypic parameters of the point cloud 3D model is evaluated by comparing the phenotypic parameters measured by manual measurement and the parameters measured by the algorithm measurement. The accuracy is evaluated based on the determination coefficient ( $R^2$ ), root mean square error (RMSE) and mean absolute percentage error (MAPE).

These formulas are as follows:

$$R^2 = \frac{\sum_{i=1}^n (X_i - \bar{X})(Y_i - \bar{Y})}{\sqrt{\sum_{i=1}^n (X_i - \bar{X})^2} \sqrt{\sum_{i=1}^n (Y_i - \bar{Y})^2}} \tag{5}$$

Where:

- $n$  is the leaf number of corn plant;
- $X_i$  is a manual measurement of phenotypic parameters;
- $\bar{X}$  is the average value of phenotypic parameters measured manually;
- $Y_i$  is the phenotypic parameter of 3D model;
- $\bar{Y}$  is the average of phenotypic parameters of three-dimensional model.

$$MAPE = \frac{1}{n} \sum_{i=0}^n \frac{|x_{ai} - x_{mi}|}{x_{mi}} \times 100\% \tag{6}$$

$$RMSE = \sqrt{\frac{1}{n} \sum_{i=0}^n (x_{ai} - x_{mi})^2} \tag{7}$$

Where:

- $MAPE$  is the average absolute percentage error;  $RMSE$  is the root mean square error;
- $n$  is the number of corn plant samples;
- $x_{ai}$  is algorithm measurement data;
- $x_{mi}$  is manual measurement data.

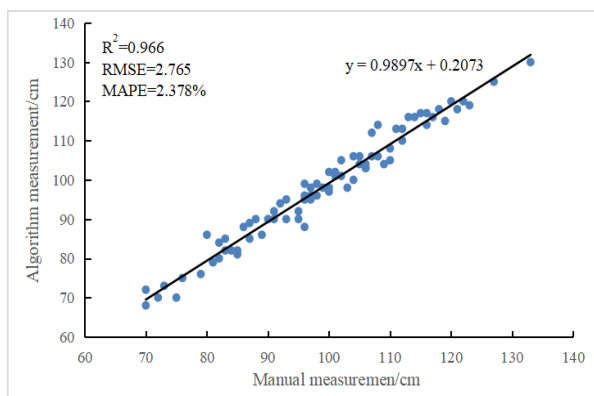


Fig. 16 - Scatter plot of comparison between manual measurement and algorithm measurement of corn plant height

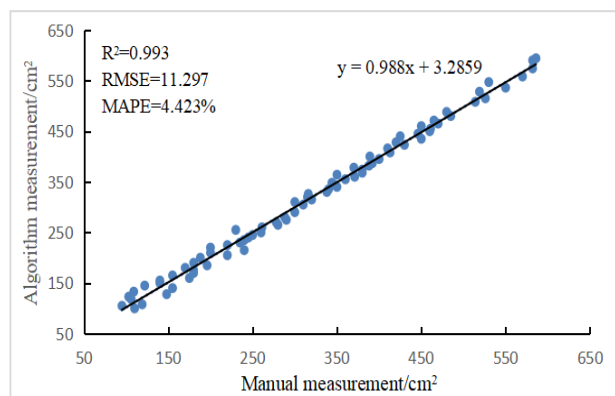


Fig. 17 - Scatter diagram of comparison between manual measurement and algorithm measurement of corn leaf area

Table 1

Comparison between manual measurement and algorithm measurement of corn stalk diameter

| Number | Long axis               |                              |                        |                    | Short axis              |                              |                        |                    |
|--------|-------------------------|------------------------------|------------------------|--------------------|-------------------------|------------------------------|------------------------|--------------------|
|        | Manual measurement / mm | Algorithmic measurement / mm | Measurement error / mm | Relative error / % | Manual measurement / mm | Algorithmic measurement / mm | Measurement error / mm | Relative error / % |
| 1      | 24.96                   | 23.03                        | 1.93                   | 7.73               | 21.56                   | 22.02                        | 0.46                   | 2.13               |
| 2      | 33.84                   | 34.44                        | 0.60                   | 1.78               | 26.59                   | 22.17                        | 4.42                   | 16.62              |
| 3      | 33.26                   | 32.51                        | 0.75                   | 2.25               | 26.11                   | 27.63                        | 1.52                   | 5.82               |
| 4      | 35.73                   | 38.36                        | 2.63                   | 7.36               | 30.49                   | 29.05                        | 1.44                   | 4.72               |
| 5      | 41.45                   | 44.17                        | 2.72                   | 6.56               | 31.16                   | 27.23                        | 3.86                   | 12.39              |
| 6      | 32.03                   | 35.65                        | 3.62                   | 11.30              | 25.01                   | 22.04                        | 2.97                   | 11.88              |
| 7      | 33.71                   | 30.76                        | 2.95                   | 8.75               | 28.67                   | 22.44                        | 6.23                   | 21.73              |
| 8      | 28.16                   | 29.53                        | 1.37                   | 4.87               | 25.61                   | 21.38                        | 4.23                   | 16.52              |



**Table 1**  
(continuation)

| Number        | Long axis               |                              |                        |                    | Short axis              |                              |                        |                    |
|---------------|-------------------------|------------------------------|------------------------|--------------------|-------------------------|------------------------------|------------------------|--------------------|
|               | Manual measurement / mm | Algorithmic measurement / mm | Measurement error / mm | Relative error / % | Manual measurement / mm | Algorithmic measurement / mm | Measurement error / mm | Relative error / % |
| 9             | 32.01                   | 25.67                        | 6.34                   | 19.81              | 25.98                   | 20.36                        | 5.62                   | 21.63              |
| 10            | 33.48                   | 41.59                        | 8.11                   | 24.22              | 23.26                   | 25.55                        | 2.29                   | 9.85               |
| 11            | 28.66                   | 26.22                        | 2.44                   | 8.51               | 21.63                   | 16.71                        | 4.92                   | 22.75              |
| 12            | 32.82                   | 43.66                        | 10.84                  | 33.03              | 27.49                   | 26.26                        | 1.23                   | 4.47               |
| 13            | 34.97                   | 37.53                        | 2.56                   | 7.32               | 25.57                   | 22.37                        | 3.20                   | 12.51              |
| 14            | 38.62                   | 38.33                        | 0.29                   | 0.75               | 27.41                   | 29.18                        | 1.77                   | 6.46               |
| 15            | 30.25                   | 31.50                        | 1.25                   | 4.13               | 26.21                   | 24.39                        | 1.82                   | 6.94               |
| 16            | 31.43                   | 33.20                        | 1.77                   | 5.63               | 23.64                   | 27.51                        | 3.87                   | 16.37              |
| 17            | 29.91                   | 30.17                        | 0.26                   | 0.87               | 24.34                   | 23.17                        | 1.17                   | 4.81               |
| 18            | 25.41                   | 30.84                        | 5.43                   | 21.37              | 22.64                   | 21.78                        | 0.86                   | 3.80               |
| 19            | 29.82                   | 28.87                        | 0.95                   | 3.19               | 24.46                   | 20.85                        | 3.61                   | 14.76              |
| 20            | 35.19                   | 31.74                        | 3.45                   | 9.80               | 23.38                   | 25.06                        | 1.68                   | 7.19               |
| Average value | 32.29                   | 33.39                        | 3.01                   | 9.46               | 25.56                   | 23.86                        | 2.86                   | 11.17              |

The algorithm and manual measurement of corn plant height are shown in Fig. 16. The determination coefficient is 0.966, the average absolute percentage error is 2.378%, the root mean square error is 2.765 cm, and the accuracy of the algorithm for measuring plant height is 97.622%. The results show that the plant height measurement method has high accuracy, and the algorithm measurement value has good consistency with the manual measurement value. The accuracy of corn leaf area is shown in Fig. 17. The determination coefficient of corn leaf area is 0.993, the average absolute percentage error is 4.423%, the root mean square error is 11.927cm<sup>2</sup>, and the accuracy of the algorithm for measuring plant height is 95.577%. The analysis results show that the algorithm measurement results are in good agreement with the two-dimensional experimental measurement results, which indicates that the algorithm measurement method of corn leaves can accurately measure the perimeter and area of corn leaves. The comparison between manual measurement and algorithm measurement of corn stem diameter is shown in Table 1. The average measurement error of the long axis of corn stem diameter is 3.01 mm, and the average measurement relative error is 9.46%. The average measurement error of the short axis of corn stem diameter is 2.86 mm, and the average measurement relative error is 11.17%. The results show that the stem extraction and measurement methods proposed in this study have high accuracy and can meet the needs of use.

## CONCLUSIONS

Based on the existing machine vision research, this paper proposes a new method of three-dimensional model reconstruction and feature segmentation for corn. Based on Kinect 2.0 combined with turntable method, corn plants are scanned to obtain corn point cloud. In the three-dimensional reconstruction of corn plants with complete information after manual rough registration and ICP fine registration, the reconstruction method improves the operation speed and measurement accuracy. The ellipse fitting and region growing segmentation algorithm for corn shape features are used to segment the characteristics of flower pot, stem and leaf. This method has high efficiency, high precision, no damage and continuous measurement. The corn plant model and the segmented corn leaves are measured. The measurement accuracy of the corn plant height algorithm is 97.622%. The average relative errors of corn stem length and short axis were 10.27% and 12.71% respectively. The measurement accuracy of corn leaf area algorithm is 95.577%. Experimental results showed that this method could extract crop phenotype parameters nondestructively and accurately. In the future, Kinect sensor is considered to be placed on a three-wheeled cart to directly collect corn information in the field. This study is of great significance for understanding crop growth status, crop detection, yield estimation and disease resistance detection.

## REFERENCES

- [1] Aksoy E. E., Abramov A., Worgotter F., et al. (2015). Modeling leaf growth of rosette plants using infrared stereo image sequences [J]. *Computers and Electronics in Agriculture*, 110:78-90.
- [2] Archibald R., Bao F., et al. (2019). A direct filter method for parameter estimation. *Journal of Computational Physics*, 398: 108871.
- [3] Ding J., Chen J., Zhou A. et al. (2019). 3D Modeling of the Rotationally Symmetric Objects Using Kinect [C]//2019 IEEE 4th International Conference on Image, Vision and Computing (ICIVC). IEEE, 685-689.
- [4] Dongyu Ren et al. (2022). A 3D reconstruction method of fruit tree branches based on Kinect v2 sensor (基于 Kinect v2 传感器的果树枝干三维重建方法) [J]. *Transactions of the Chinese Society for Agricultural Machinery*, 53(S2):197-203.
- [5] Gang Liu, Yohan Yin et al. (2022). Cherry canopy denoising and registration method based on three-dimensional point cloud (基于三维点云的群体樱桃树冠层去噪和配准方法). *Transactions of the Chinese Society of Agricultural Machinery*. 1-11.
- [6] He JQ, Ha Rison R.J. et al. (2017). A novel 3D image system for strawberry phenotyping [J]. *Plant Methods*, 13(1):1-8.
- [7] Hui F., Zhu J., Hu P. et al. (2018). Image-based dynamic quantification and high-accuracy 3D evaluation of canopy structure of plant populations. *Annals of Botany*, 121(5): 1079-1088.
- [8] Hui Chen, Tingting Wang et al. (2021). Three-dimensional Measurement Method of Leaf Area of Irregular Plants Based on Motion Restoring Structure (基于运动恢复结构的无规则植物叶片面积三维测量方法). *Transactions of the Chinese Society of Agricultural Machinery*. 52(04): 230-238.
- [9] Jay S., Rabatel G., Hadoux X., et al. (2015). Infield crop row phenotyping from 3D modelling performed using structure from motion. *Computers and Electronics in Agriculture*, 110: 70-77.
- [10] Jin Zhou et al. (2013). Fast reconstruction of 3D human body using Kinect (使用 Kinect 快速重建三维人体) [J]. *Journal of Computer Aided Design and Graphics*, 25(6): 873-879.
- [11] Qian Wu. (2022). *Segmentation and registration of citrus point cloud based on Kinect v2 camera (基于 Kinect v2 相机的柑橘点云分割与配准研究)* [D].Guangxi Normal University. DOI:10.27036/d.cnki.ggxsu.2022.001585.
- [12] Song Bi, Yuhao Wang, (2021). LiDAR point cloud denoising method based on adaptive radius filter (基于自适应半径滤波的农业导航激光点云去噪方法研究) [J]. *Transactions of the Chinese Society for Agricultural Machinery*, 52(11): 234-243.
- [13] Wu D., Ye J.L., Wang K. et al. (2020) Research on 3D reconstruction method of potted rice based on contour projection [J]. *Agric. Sci. Technol.*, 22:87-95.
- [14] Xiong X., Yu L., Yang W., et al. (2017). A high-throughput stereo-imaging system for quantifying rape leaf traits during the seedling stage. *Plant Methods*, 13(1): 1-17.
- [15] Xu Wu, Luling Wen, Dongdong Liang et al. (2019), Comparative Study of Surface Reconstruction Algorithms Based on Point Cloud Data (基于点云数据的曲面重建算法比较研究), *Journal of Anhui Normal University (Natural Science Edition)*, 042(001): 46-50.
- [16] Yingbo Song, Wei Guo, Hongquan Zhang, et al. (2015). Practical application of image processing techniques for measuring leaf area of corn (图像处理技术在玉米叶面积测量中的实际应用). *Journal of Agriculture*, 5(8): 111-114.
- [17] Yaochen Li. (2019). *Measurement of Morphological Characteristics of Cotton Seedlings Based on Structured Light Imaging (基于结构光成像的棉花幼苗形态特征测量)*. Huazhong Agricultural University.
- [18] Zila Jia, Yungang Bai, Biao Cao, (2019), Effects of different water treatments on plant growth and yield of silage corn under mulched drip irrigation in northern Xinjiang (北疆寒旱区不同水分处理对膜下滴灌青贮玉米植株生长与产量的影响). *Chinese Agricultural Science Bulletin*, 35(16): 6-14.